STUDIA UBB CHEMIA, LXVII, 4, 2022 (p. 261-272)
(RECOMMENDED CITATION)
DOI:10.24193/subbchem.2022.4.17

STUDY ON THE CORROSION INHIBITION EFFICIENCY OF ALUMINUM TRIPOLYPHOSPHATE ON ZINC SUBSTRATE

Julia BOTH[a], Gabriella SZABÓ[b*], Liana-Maria MUREȘAN[a]

ABSTRACT. The aim of the present study was the electrochemical investigation of the inhibition efficiency of aluminum-tripolyphosphate (ATPP) incorporated in silica (SiO_2) and chitosan (Chit) coatings prepared on zinc substrates. Coatings were prepared by dip-coating method. Electrochemical characterization of the coatings was performed by using electrochemical impedance spectroscopy (EIS) and potentiodynamic polarization curves (PDP). Effect of ATPP on Zn was also determined in 0.2g/L Na_2SO_4 solution and its adsorption on zinc was studied. Results concluded that the ATPP adsorption on Zn obeys Langmuir isotherm. The best corrosion resistance was reached when Zn was protected by SiO_2 coating, obtained from a precursor sol containing 10^{-3} M ATPP.

Keywords*: zinc; silicon dioxide; chitosan; Al-tripolyphosphate; anti-corrosion coating; adsorption.*

INTRODUCTION

Corrosion has been one of the main global issues of the century. With ever-advancing technologies, the most effective use and protection of all metal types and structures is of vital importance in order to obtain effective and lasting systems. The most common methods of corrosion prevention include the production of metal alloys, the use of inhibitors, or the application of anti-corrosive barrier coatings. Though highly effective, previously greatly

---

[a] *Babeş-Bolyai University, Faculty of Chemistry and Chemical Engineering Department of Chemical Engineering, 11 Arany Janos str., RO-400028, Cluj-Napoca, Romania.*

[b] *Babeş-Bolyai University, Faculty of Chemistry and Chemical Engineering, Department of Chemistry and Chemical Engineering of Hungarian Line, 11 Arany Janos str., RO-400028, Cluj-Napoca, Romania.*

* *Corresponding author: gabriella.szabo@ubbcluj.ro.*

demanded chromate inhibitors were excluded due to their high toxicity and carcinogenic nature [1], thus leaving the industry with a high demand for similarly effective alternatives. Developed for this sole purpose, both organic and inorganic coating systems have been previously reported in scientific literature.

Organic and hybrid polymer-based substances are the most commonly used as anti-corrosion barrier coatings, due to their versatility and resilience [2]. Examples of such studied organic coatings are paints [3], epoxy-[4], polystyrene-[5], —and a more environmentally friendly option— chitosan-[6, 7]. Chitosan, as a corrosion protective agent, was reported, along with its derivates and composites for the corrosion protection of steel alloys [8], as self-healing barrier coating in the case of 2024 aluminum alloy [9], even as smart coating [10] and nanocontainers for antimicrobial applications [11]. Chitosan (Chit) is a great alternative for peelable and temporary coating systems for industrial use [12].

Inorganic materials, such as silica (SiO_2) [13, 14], were also thoroughly studied due to their durability and high resistance to the corrosive environment [15]. Silica nanoparticles were used as carriers for the encapsulation of corrosion inhibitors [16, 17] in different coating matrices for the development of smart coatings. The introduction of different functional groups *via* additives and inhibitors into the inorganic silica matrix was proven to aid corrosion resistance, while also enhancing mechanical and physical properties [18]. Thus, compact [19] and mesoporous [20] silica coatings loaded with a variety of organic inhibitors (e.g., tannic acid [21], benzotriazole, and cetyltrimethylammonium bromide [22, 23]) were rigorously investigated.

Aluminium-tripolyphosphate (ATPP) is a layered, inorganic compound with a wide application spectrum, due to its capacity to intercalate other compounds into its structure [24]. It is most commonly used as an anti-corrosion pigment or precursor for other corrosion inhibitors, due to its low toxicity [25] and low production costs [26]. ATPP also acts as a rust-converter, showing great compatibility with different resins [27]. Studies on ATPP were mostly conducted on steel substrates. Significant studies on the effects of ATPP on zinc plates are yet to be reported.

The aim of the current study was primally the determination of the inhibition efficiency of ATPP in 0.2g/L Na_2SO_4 solution and after incorporation in two different coating types — an inorganic one, SiO_2, and biopolymer, Chit — on zinc substrates. It is worth mentioning, that the mechanical properties (roughness, porosity, etc.) of the used metal substrates can potentially affect the behavior of the applied coatings. Based on previous studies, ATPP was introduced directly into the SiO_2 sol before the coating preparation [21], while for Chit coatings, ATPP was introduced *via* impregnation [6, 28], The prepared coatings were characterized by electrochemical impedance spectroscopy (EIS) and potentiodynamic polarization curves (PDP). A pre-assessment of the adsorbtion of different ATPP concentrations on the zinc wafer was determined by using Langmuir's isotherm, which was calculated with the use of Rp values deducted from EIS spectra [29].

RESULTS AND DISCUSSION

The inhibition effect of aluminum tripolyphosphate (ATPP) was studied either dissolved in Na_2SO_4 aqueous solutions, or after its incorporation in SiO_2 or Chitosan coatings. In all cases, Zn was the used substrate.

Effect of ATPP in aqueous solutions on Zn corrosion

In order to observe if the ATPP presents any corrosion inhibition efficiency, aqueous Na_2SO_4 solutions of pH 5 containing this compound were prepared in a wide concentration range. The effect of the different solutions on the Zn plates was studied by means of electrochemical methods, by both potentiodynamic polarization (PDP) and electrochemical impedance spectroscopy (EIS) measurements. First of all, the polarization curves of the different samples were recorded (**Figure 1**) and the corrosion current densities were determined by Tafel interpretation method (**Table 1**).

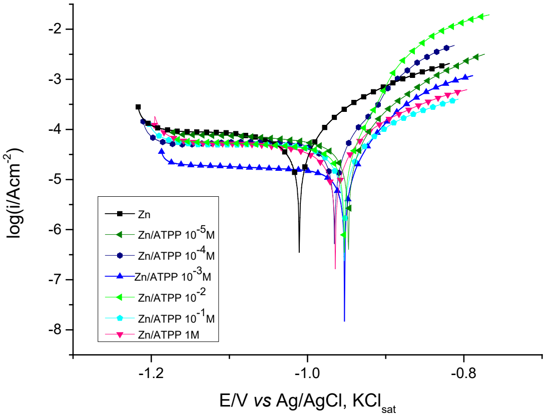

Figure 1. Anodic and cathodic polarization curves for Zn in 0.2 g/L Na_2SO_4(pH=5) blank solution and in Al tripolyphosphate containing solution in 1M-10^{-5} M concentration range.

It can be easily observed from the polarization curves, that in the case of extreme concentrations (1M, 10^{-1}M, and 10^{-5}M) the curves are very closely situated one from another, and their position is only slightly lower than that corresponding to Zn in the solution without inhibitor. This fact is reflected in the values of the corrosion current densities too (**Table 1**). On the contrary, in solutions having the ATPP concentration in the middle of this interval, a greater inhibition effect was noticed, leading to the conclusion that there is an optimal concentration range for ATPP as a corrosion inhibitor. As it can be seen from **Figure 1**, mostly the anodic branches are affected by the inhibitor, due to the adsorption of the ATPP on zinc and blocking of the metal surface. The results are not spectacular but suggest clearly that ATPP acts mainly as an anodic inhibitor. Moreover, in all cases when the inhibitor was present in the solution, can be observed a shift of the E_{corr} toward positive values. This could be explained by the increased control degree of the anodic reaction— the metal dissolution, on the global process.

The efficiency of the inhibition (IE), determined from PDP measurements, was calculated with the following Equation (1):

$$IE\% = \frac{i_{corr}^{o} - i_{corr}}{i_{corr}^{o}} \times 100 \qquad (1)$$

where i_{corr}^{o} and i_{corr} represent the corrosion current densities in solutions without and with ATPP content, respectively.

Table 1. Kinetic parameters obtained from the potentiodynamic polarization curves of the Zn samples immersed in ATPP aqueous solution

Sample	i_{corr} µAcm^{-2}	E_{corr} V *vs* Ag/AgCl,KCl$_{sat}$	b_c V/dec	b_a V/dec	IE %
Zn	62.18	-1.011	0.686	0.090	
Zn/ATPP-1M aq	40.68	-0.964	0.982	0.114	34.6
Zn/ATPP-10^{-1} M aq	39.76	-0.953	0.724	0.127	36.1
Zn/ATPP-10^{-2} M aq	34.51	-0.952	0.442	0.038	44.5
Zn/ATPP-10^{-3} M aq	13.24	-0.952	0.844	0.044	78.7
Zn/ATPP-10^{-4} M aq	33.37	-0.965	0.223	0.058	46.3
Zn/ATPP-10^{-5} M aq	50.68	-0.947	0.734	0.075	18.5

In order to get a more accurate image of this phenomenon and aiming to examine the inhibitor adsorption, EIS measurements were performed in a narrower concentration interval. The impedance spectra were recorded at open circuit potentials in the 10 kHz – 10 mHz frequency range. The obtained Nyquist diagrams are presented in **Figure 2**.

The capacitive loop of the Nyquist spectra is attributed to the polarization resistance, including a major contribution of the charge transfer resistance.

It can be observed, that at low concentrations (10^{-5} M) the spectrum is almost the same as that of Zn in absence of the inhibitor. With the increase of the ATPP concentration, the diameter of the loop is increasing, reaching the maximum at 10^{-3} M, and after that it decreases again.

It is worth mentioning that these results are in agreement with the polarization measurements, pointing out the optimal concentration of ATPP of 10^{-3} M. Also, the values of IE (calculated from the corrosion current densities) and z (the inhibition efficiency percentage) that indicates the effectiveness of the inhibition determined from the polarization resistance (equation 3 and 4), are very close to each other.

The possible mechanism reported in the literature is based on the capacity of aluminium triphosphate to release phosphates, which then form a protective layer on the metal substrate, impeding the access of the aggressive species and hindering metal corrosion [30].

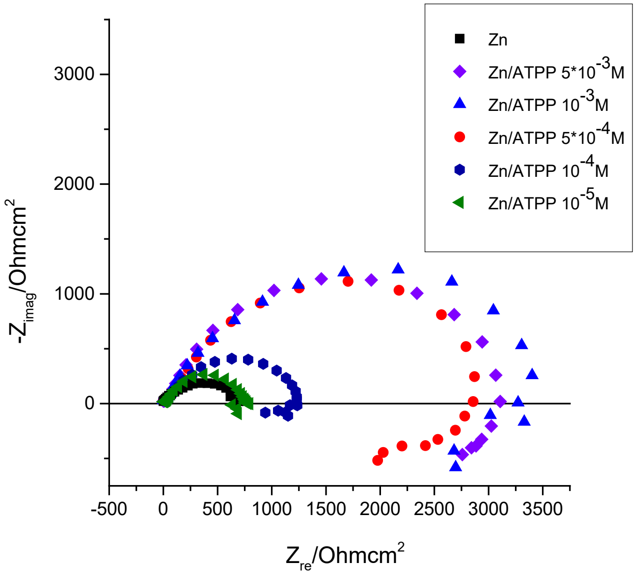

Figure 2. Nyquist spectra for Zn in 0.2 g/L Na_2SO_4(pH=5) blank solution and in Al tripolyphosphate containing solution in $5 \cdot 10^{-3}$-10^{-5} M concentration range.

As already mentioned, the increase of the polarization resistance and, consequently, of the corrosion inhibition is due to the adsorption of the ATPP on Zn, therefore it is important to find the isotherm that fits the experimental data. The first isotherm that was taken into consideration was the Langmuir isotherm. The linear form of the Langmuir isotherm is given by Equation (2):

$$\frac{c_{ATPP}}{\theta} = \frac{1}{K} + c_{ATPP} \quad (2)$$

where the θ represents the surface coverage, K is the adsorption constant, and c_{ATPP} is the concentration of the inhibitor. The surface coverage can be calculated from the impedance spectra with Equation (3):

$$\theta = \frac{R_p - R_p^0}{R_p} \quad (3)$$

The R_p and R_p^o are the polarization resistance of solutions containing inhibitor and without it respectively. The inhibition efficiency percentage, calculated from EIS data, can be calculated with Equation (4):

$$z = 100 \times \theta\ [\%] \quad (4)$$

The adsorption constant, K was calculated with Equation (5):

$$K = \frac{1}{55.5} exp\left(\frac{-\Delta G_{ads}^0}{RT}\right) \quad (5)$$

In this equation, 55.5 stands for the molar concentration of water expressed in mol/dm^3, R represents the universal gas constant, and T is the thermodynamic temperature. The determined adsorption parameters extracted from the impedance diagrams taking into account the Langmuir isotherm are summarized in **Table 2**.

Table 2. Adsorption parameters obtained from the Nyquist spectra of the Zn samples immersed in ATPP aqueous solution

C_{TPP}/M	R_p/Ω·cm^2	θ	$10^3 \cdot C_{TPP}/\theta$ M	z %	K M^{-1}	ΔG_{ads} kJ/mol
0	743	0	0		$16.16 \cdot 10^3$	-33.96
10^{-5}	815	0.088	0.11	8.0		
10^{-4}	1253	0.407	0.24	40.7		
$5 \cdot 10^{-4}$	2859	0.740	0.67	74.0		
10^{-3}	3342	0.777	1.29	77.7		
$5 \cdot 10^{-3}$	3100	0.760	6.58	76.0		

The validity of Langmuir isotherm can be noticed on **Figure 3**, which fits the experimental data with high accuracy (R^2 = 0.9995).

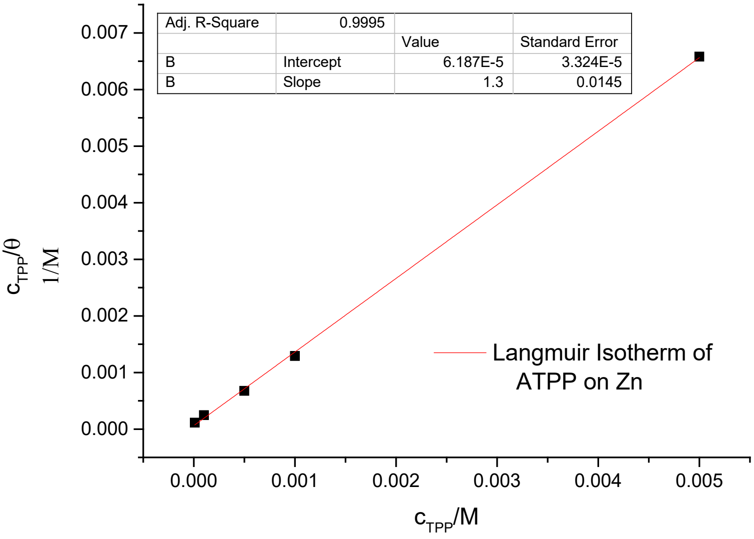

Figure 3. Aluminium tripolyphosphate adsorption from aqueous solutions on Zn substrate: Langmuir isotherm

In general terms, the free energy value determined from Equation (5) can inform about the nature of adsorption: whether it is only physical adsorption ($\Delta G_{ads.}^{o}$>-20 kJ/mol) or the process is accompanied by chemical bond formation (chemisorption) [31] when $\Delta G_{ads.}^{o}$<-40 kJ/mol. Taking into account the value obtained in our case, chemical bond formation between the inhibitor molecules and the substrate is unlikely.

Effect of ATPP incorporated in chitosan coating on Zn

Chitosan is a remarkable, wide used biopolymer in several industry branches because of its biodegradability, antibacterial properties, and bioavailability. Regardless of the many useful properties, its permeability is sometime inconvenient. Due to the pseudo-porosity of the chitosan thin layers the corrosive electrolyte species can easily reach the metal surface and consequently facilitate the dissolution process. Therefore, the remediation of this disadvantage is frequently obtained through chemical modification by impregnation technique. The positive charge of Chit and the negative charge of ATPP are a good starting point for creation of a consolidated coating with protective properties.

The Chit coated Zn samples were impregnated with 10^{-3} M ATPP aqueous solution, after this had proven to be the most effective incorporation method. The inhibitor was introduced in the layer by immersion for different time intervals. EIS measurements were performed on the chemically modified and dried coatings.

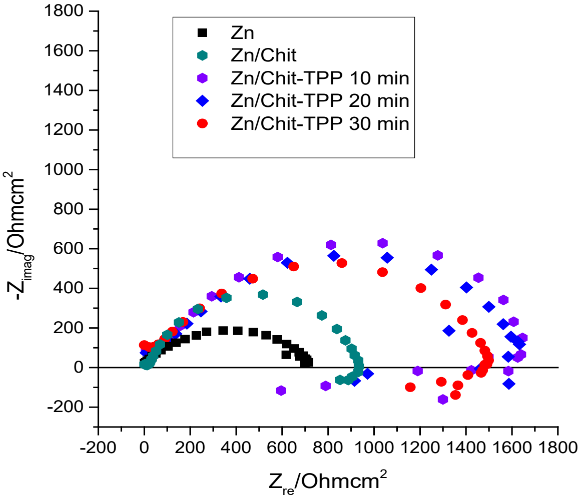

Figure 4. Nyquist spectra for Chit coated Zn impregnated for 10 min, 20 min and 30 min with 10^{-3} M Al tripolyphosphate agueous solution, recorded in 0.2 g/L Na_2SO_4 (pH=5).

The recorded spectra are depicted in **Figure 4**. It can be observed, that: (i) in all cases the impregnation caused an increased polarization resistance; (ii) the optimal effect was reached with immersion for 10 min. An explanation of this inhibition effect can consist of the cross-linking of the Chit by the ATPP, due to the interaction between the protonated NH_2 groups of Chit and phosphate anions [32].

Effect of ATPP incorporated in SiO_2 coating on Zn

The beneficial effect of Aluminum-tripolyphosphate was also tested using an inorganic matrix, — silica coating.

In this case, the different amounts of ATPP were introduced in the precursor sol. EIS measurements were performed on the coated Zn samples. The obtained impedance spectra are presented in **Figure 5**.

The polarization resistance values are all larger than in the case of chitosan coatings, even without any inhibitor. This points out to better barrier properties of silica coatings, as compared with the chitosan ones. Moreover, even though both SiO_2 and ATPP are negatively charged, their combination led to a coating with higher resistance. This could be due to an insertion of phosphate ions in the silica network during the sol formation.

As it can be observed the best effect was provided by both coatings (SiO_2 and Chit) with 10^{-3} M ATPP content.

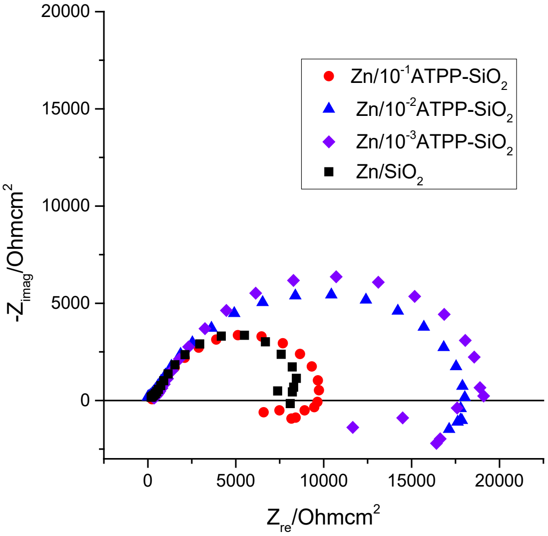

Figure 5. Nyquist spectra for SiO_2 coating doped with 10^{-1}M, 10^{-2}M and 10^{-3} M Al tripolyphosphate on Zn, recorded in 0.2 g/L Na_2SO_4 (pH=5).

It is of great importance to mention, that SiO_2 and Chit coatings offer different uses and advantages: while SiO_2 has higher durability and resilience and thus can present as a permanent solution, Chit is also a great alternative for temporary systems. Both of these are of great use in the industry of corrosion protection, hence why, the fact that ATPP can be introduced in both coating systems offers a valuable information from a practical point of view.

CONCLUSIONS

ATPP inhibition effect was studied on Zn substrate. In aqueous solution containing ATPP, it was observed the existence of an optimal concentration (10^{-3}M) that provides the highest corrosion current density decrease.

By examining the potentiodynamic polarization curves one can conclude, that the inhibition effect is visible mostly on the anodic branch and affects the metal dissolution process. The calculated standard free energy value allows us to conclude, that predominantly physical adsorption takes place.

ATPP kept its corrosion inhibitor properties even when it was introduced in two different types of coatings (inorganic or biopolymer), with different techniques (mixed in the precursor sol or impregnated from its solution).

The best corrosion resistance was reached when Zn was protected by SiO_2 coating prepared from a precursor containing 10^{-3} M ATPP.

EXPERIMENTAL SECTION

Materials

Natural zinc plates of 2x6x0.55 cm were used as the metal substrate for the applied coatings. Pre-treatment of the substrates was obtained with 0.1M HCl (37%, Merck) aqueous solution and 2-propanol (pure, Chempur).

Precursor sol of SiO_2 was prepared with ethanol (99.3%, Chemical Company), tetraethoxysilane (TEOS, 98%, Alfa-Aesar) and 0.1M HCl (37%, Merck) aqueous solution. Chit solution was prepared with medium molecular weight chitosan (Sigma-Aldrich) and 1% acetic acid (99.5%, Chemical Company) aqueous solution. ATPP (Bridgexim) inhibitor was introduced into both of the coating systems. 0.2 g/L Na_2SO_4 (99%, Sigma-Aldrich) aqueous solution was used as electrolyte medium to carry out electrochemical measurements.

Pretreatment of the zinc plates

Zinc substrates were subjected to a thorough pre-treatment process prior to the application of the prepared precursors. Firstly, the plates were carefully sanded with emery paper (P800, P1500, P2000, P3000, P5000), which was then followed by a surface treatment applied with 0.1M HCl solution, rinsed with distilled water and then degreased with 2-propanol.

Preparation of SiO_2 and Chit precursors

Different, sequential amounts of ATPP were introduced into the SiO_2 sols. The sols were prepared by blending of 20 mL ethanol and 7 mL TEOS with the addition of 10^{-3} M, 10^{-2} M and 10^{-1} M ATPP in a beaker. Concentrations were calculated with the total volume of a SiO_2 sol/batch. The mixture was stirred under standard conditions for 1 hour at 400 rpm. After 1 hour a mixture of 2ml ethanol, 2 mL TEOS and 4 mL .01M HCl was added to the beaker and left under agitation for an additional hour. Chit solution was prepared from the mixture of 1% aqueous acetic acid and 1g of medium molecular weight chitosan which was then agitated for 24 hours.

Preparation of the coatings

Coatings were prepared by dip-coating method with a home-made dip-coater. SiO_2 layers were prepared with a 12 cm/min dipping speed [21], while Chit layers were prepared with a 5 cm/min dipping speed [7]. SiO_2 coatings were thermally treated for 1 hour at 150°C. Chit layers were left to air-dry for 24 hours. After that the impregnation of the Chit coatings was performed by dip-coating technique. The Chit coated samples were immersed in 1mM aqueous ATPP solution with 12 cm/min dipping speed, kept in solution for 10 min, 20 min and 30 min respectively, then withdrawn with the same 12 cm/min speed [28]. Finally, after withdrawal the excess of inhibitor was washed off with distilled water and the samples were dried.

Electrochemical evaluation of prepared coatings

Electrochemical characterization of the coatings was obtained by OCP, EIS and PDP measurements, which were performed in a three electrode cell on a PARSTAT-2273 potentiostat.

The three electrode cell contained a working electrode (WE- bare or coated zinc substrates), a counter electrode (CE- platinum wire) and a reference electrode (RE- Ag/AgCl/KCl_{sat}). 0.2g/L Na_2SO_4 aqueous solution was used as electrolyte solution.

OCP measurements were carried out for 1h each until the stabilisation of the coated and bare metal plates in the electrolyte solution, in order to obtain a E_{corr} (corrosion potential) as a reference value for further analyses. EIS measurements were carried out in a 10 mHz– 10 kHz frequency interval, with a sinusoidal current of 10 mV amplitude. PDP measurements were carried out at E=±200mV vs.OCP, at a scan rate of 1 mV/min.

ACKNOWLEDGMENTS

Julia Both thanks the Romanian Ministry of Education for the financial support of her doctoral studies.

REFERENCES

1. R.M. Park, J.F. Bena, L.T. Stayner, R.J. Smith, H.J. Gibb, P.S.J. Lees, *Risk Anal.*, **2004**, *24*, 1099–1108
2. S.B. Lyon, R. Bingham, D.J. Mills, *Prog. Org. Coat.*, **2017**, *102(A),* 2-7
3. J. Both, R. Mezei, G. Szabó, L. M. Mureșan, *Prot. Met. Phys. Chem.*, **2022***, 58(4),* 822–833
4. K. Saravanan, S. Sathiyanarayanan, S. Muralidharan, S. Syed Azim, G. Venkatachari, *Prog. Org. Coat.*, **2007**, *59(2)*, 160–167
5. J. Both, G. Szabó, G. Katona, L.M. Mureșan, *J. Electrochem. Sci,* **2022**, *12(4)*
6. Á.F. Szőke, G. Szabó, Z. Hórvölgyi, E. Albert, L. Gaina, L.M. Muresan, *Carbohydr. Polym.*, **2019**, *215*, 63–72

7. Á.F. Szőke, G. Szabó, Z. Simó, Z. Hórvölgyi, E. Albert, A.G. Végh, L. Zimányi, L.M. Muresan, *Eur. Polym. J.*, **2019**, *118*, 205–212
8. H. Ashassi-Sorkhabi, A. Kazempour, *Carbohydr. Polym.*, **2020**, *237*, 116110
9. J. Carneiro, J. Tedim, S.C.M. Fernandes, C.S.R. Freire, A.J.D. Silvestre, A. Gandini, M.G.S. Ferreira, M.L. Zheludkevich, *Prog. Org. Coat.*, **2012**, *75(1–2),* 8–13
10. J. Carneiro, J. Tedim, M.G.S. Ferreira, *Prog. Org. Coat.*, **2015**, 89, 348–356
11. A.F. Bettencourt, C. Tomé, T. Oliveira, V. Martin, C. Santos, L. Gonçalves, M.H. Fernandes, P.S. Gomes, I.A.C. Ribeiro, *Carbohydr. Polym.,* **2021**, *254*, 117433
12. E. Luckachan, V. Mittal, *Corros. Sci. Technol.*, **2016**, *15(5)*, 209–216
13. W.J. van Ooij, D. Zhu, V. Palanivel, *et al., Silicon Chem*, **2006**, *3*,11–30.
14. T.R. Ovari, G. Katona, G. Szabo, L. M. Muresan, *Studia UBB Chemia*, **2022**, *67(1)*, 227–244
15. I.S. Bayer, *Coatings*, **2017**, *7*, 12
16. M Yeganeh, M. Omidi, S.H.H. Mortazavi, A. Etemad, M.H. Nazari, S.M. Marashi, *MNT*, **2020**, 275–294
17 J.M. Falcón, F.F. Batista, I.V. Aoki, *Electrochim. Acta*, **2014**, *124*, 109–118
18. C.A. Milea, C. Bogatu, A. Duta, *Bull. Trans. Univer. Braşov ser. I Eng. Sci.,* **2011***, 4(53)*
19. E. Volentiru, M. Nyári, G. Szabó. Z. Hórvölgyi, L.M. Mureșan, *Period. Polytech. Chem. Eng.*, **2014**, *58(Supplement)*, 61–66
20. E. Albert, N. Cotolan, N. Nagy, Gy. Sáfrán, G. Szabó, L.M. Mureşan, Z. Hórvölgyi, *Micropor. Mesopor. Mater.*, **2015**, *206,* 102–113
21 J.Both, G. Szabó, G. Katona, L.M. Muresan, *Mater. Chem. Phys.*, **2022**, *282*, 125912
22. G. Szabó, E. Albert, J. Both, L. Kócs, Gy. Sáfrán, Á.F. Szőke, Z. Hórvölgyi, L.M. Mureşan, *Surf. Interfaces.,* **2019**,*15*, 216–223
23. N. Cotolan, S. Varvara, E. Albert, G. Szabó, Z. Hórvölgyi, L.M. Muresan, *Corros. Eng. Sci. Tech.,* **2016**, *51(5)*, 373–382
24. C. Hejjaj, A. Ait Aghzzaf, I. Bouali, R. Hakkou, M. Dahbi, C.B. Fischer, *Corros. Sci.*, **2021**, *181*,109239
25. A. Khadiri, R. Saddik, K. Bekkouche, A. Aouniti, B. Hammouti, N. Benchat, M. Bouachrine, R. Solmaz, *J. Taiwan Inst. Chem. Eng.*, **2016**, *58,* 552–556
26. A. AïtAghzzaf, B. Rhouta, E. Rocca, A. Khalil, J. Steinmetz, *Corros. Sci.*, **2014**, *80*, 46–52
27. W. Li, Z. Fan, X. Li, B. Jiang, F. Yan, Z. Zhang, X. Wang, Prog. Org. Coat., **2019**, *135*, 483–489
28. P. Márton, E. Albert, N. Nagy, B. Tegze, G. Szabó, Z. Hórvölgyi, *Studia UBB Chemia*, **2020**, *65(3)*, 63–79
29. R. Bostan, S. Varvara, L. Găină, L.M.J. Mureșan, *Corros. Sci.*, **2012**, *63*, 275–286
30. D. Song, J. Gao, L. Shen, H. Wan, and X. Li, *J. Chem.*, **2015**, *2015*
31. D.Q. Zhang, Q.R. Cai, X.M. He, L.X. Gao, G.D.J. Zhou, *Mater. Chem.*, **2008**, *112(2)*, 353–358
32. Z. Cui, Y. Xiang, J. Si, M. Yang, Q. Zhang, T.J. Zhang, *Carbohydr. Polym.*, **2008**, *73(1)*, 111–116